Interplay between out-of-plane magnetic plasmon and lattice resonance for modified resonance lineshape and near-field enhancement in double nanoparticles array*

Ding Pei(丁 佩)[a)†], Wang Jun-Qiao(王俊俏)[b)], He Jin-Na(何金娜)[b)], Fan Chun-Zhen(范春珍)[b)], Cai Gen-Wang(蔡根旺)[b)], and Liang Er-Jun(梁二军)[b)]

[a)] *Department of Mathematics and Physics, Zhengzhou Institute of Aeronautical Industry Management, Zhengzhou* 450015, *China*
[b)] *School of Physical Science and Engineering and Key Laboratory of Materials Physics of Ministry of Education of China, Zhengzhou University, Zhengzhou* 450052, *China*

(Received 21 February 2013; revised manuscript received 19 April 2013)

Two-dimensional double nanoparticle (DNP) arrays are demonstrated theoretically, supporting the interaction between out-of-plane magnetic plasmons and in-plane lattice resonances, which can be achieved by tuning the nanoparticle height or the array period due to the height-dependent magnetic resonance and the periodicity-dependent lattice resonance. The interplay between the two plasmon modes can lead to a remarkable change in resonance lineshape and an improvement on magnetic field enhancement. Simultaneous electric field and magnetic field enhancement can be obtained in the gap region between neighboring particles at two resonance frequencies as the interplay occurs, which presents "open" cavities as electromagnetic field hot spots for potential applications on detection and sensing. The results not only offer an attractive way to tune the optical responses of plasmonic nanostructure, but also provide further insight into the plasmon interactions in periodic nanostructure or metamaterials comprising multiple elements.

Keywords: magnetic plasmon, lattice resonance, field enhancement, nanoparticles array

PACS: 78.67.Pt, 42.25.Bs, 78.20.Bh, 73.20.Mf **DOI:** 10.1088/1674-1056/22/12/127802

1. Introduction

Metal nanostructures with their optical responses governed by the localized surface plasmon resonances (LSPR) have drawn a great deal of attention over the past decades due to the ability to confine sub-wavelength and enhance the intensity of the optical field.[1–4] In recent years, the coupling of two or more simple plasmonic structures has been extensively studied to achieve new and enhanced optical properties based on surface plasmons because the interaction between different plasmon modes enables spatial redistribution of the electromagnetic energy and great modification of the spectral characteristic.[5] One of the coupling systems studied most is metallic nanoparticle (NP) dimer, such as pair of nanospheres,[6] nanodisks,[7] nanocubes,[8] nanorods,[9] nanoshells,[10] nanorings,[11] etc. Each of them exhibits a large spectral shift with respect to the LSPR of individual NPs and a huge enhancement of the local electric field in the gap between two NPs, being strongly dependent on the NP's composition, shape, size, relative orientation, interparticle distance, and dielectric environment.[9,12–14] Another effect of great interest is the occurrence of magnetic resonance in some specially shaped NP pairs, which are characterized by circulating displacement currents that couple strongly to the incident magnetic field.[15,16] Intense and tunable optical magnetism at visible frequencies has potential applications in cloaking, super-resolution imaging, and ultrasensitive chemical and biological sensors.[17–19]

On the other hand, periodic arrays of metallic nanostructures become one of the objects of scientific interest due to their optical responses being dramatically different from those of isolated NPs, especially when the grating order is transformed from radiative to evanescent.[20–22] Recently, theoretical and experimental investigations demonstrated that the strong coupling between the LSPR of nanostructures and the grating diffraction (i.e., Rayleigh anomalies) in a two-dimensional (2D) array can excite narrow lattice plasmon resonances by suppressing radiative loss,[22–26] which possesses a much higher quality factor Q and exhibit promising applications in field enhancement, polarized light emission, and sensing.[27,28]

In this paper, we investigate the interaction between the in-plane lattice resonance and the out-of-plane magnetic resonance that arises from the plasmon coupling of two adjacent NPs in a 2D double nanoparticle (DNP) array. This kind of

*Project supported by the National Natural Science Foundation of China (Grant Nos. 10974183, 11104252, 61274012, and 51072184), the Specialized Research Fund for the Doctoral Program of Higher Education of China (Grant No. 20114101110003), the Aeronautical Science Foundation of China (Grant No. 2011ZF55015), the Basic and Frontier Technology Research Program of Henan Province, China (Grant Nos. 112300410264 and 122300410162), the Foundation of University Young Key Teacher from Henan Province, China (Grant No. 2012GGJS-146), the Key Program of Science and Technology of Henan Education Department, China (Grant Nos. 12A140014 and 13A140693), and the Postdoctoral Research Sponsorship of Henan Province, China (Grant No. 2011002).

†Corresponding author. E-mail: dingpei@zzia.edu.cn

© 2013 Chinese Physical Society and IOP Publishing Ltd

magnetic resonance in nanoparticle pairs has been reported, but the interaction with the lattice resonance has not been investigated yet.[16] Comparing with previous work in which the changes in in-plane architecture (lattice spacing, NP size, NP shape, interparticle distance, etc.) were used to tune the optical response of the dimers, we indicate that the resonance wavelength of the out-of-plane magnetic plasmon can be tuned simply by changing the NP height, without changing the overall geometry of the nanostructures. By controlling the out-of-plane magnetic plasmon via NP height or tuning the in-plane lattice resonance through array period, the interaction between them can be achieved, which not only leads to a remarkable transition of the transmittance lineshape from one resonance dip to two dips in the considered wavelength range, but also results in an improvement of magnetic field enhancement. As a result, the gaps between neighboring NPs become hot spots of electric field and magnetic field, simultaneously, at two resonance wavelengths. Different from previous reports on achieving magnetic field enhancement through "stacked" rod pairs or disk pairs,[15,29,30] the planar DNPs can provide "open" cavities for the excitation and detection of magnetic transitions in atoms and molecules, showing the potential applications of magnetic nonlinearity and magnetic sensors.[17–19]

2. Structure and simulation method

The DNP array is shown schematically in Fig. 1(a), where two cylindrical gold NPs with the same shape and size are arranged in a square lattice on a silica glass. The periods in x and y directions are both set to be $h = 470$ nm. The NP radius and the edge-to-edge separation between two adjacent particles are fixed to be $r = 60$ nm and $g = 25$ nm, respectively. The NP height h varies from 60 nm to 160 nm in steps of 10 nm.

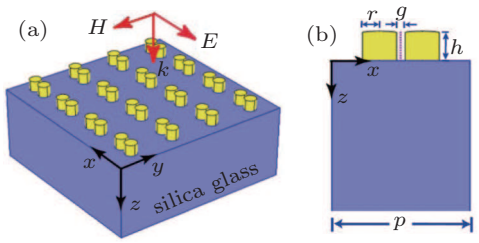


Fig. 1. (color online) (a) Schematic diagram of a 2D square array of two cylindrical gold NPs placed on a silica glass, with the incident light polarization defined. (b) Side view of a unit cell in the DNP array, where the structural parameters of p, r, g, h represent the periodicity, NP radius, interparticle distance, and NP height, respectively. The red dashed line between two particles shows the integration path for calculating the averaged electromagnetic field enhancement factor.

Numerical electromagnetic simulations were performed in Comsol Multiphysics 4.2 with the RF module. The computational domain only contained a unit cell as shown in Fig. 1(b), where periodic boundary conditions were employed for four lateral boundaries and perfectly matched layers (PML) were used in the propagation direction to eliminate the non-physical reflections at the domain boundaries. The cell was meshed with tetrahedral elements and the local mesh refinement with size less than 5 nm was used around the NPs. A plane wave with the incident direction perpendicular to the array plane and the polarization direction parallel to the dimer axis, irradiated the top of the unit. The refractive index of silica glass was set to be 1.45 and an experimentally measured dielectric function of gold was utilized in the simulations.[31] To obtain the transmission and extinction spectra, the output power was integrated at the bottom boundary in a wavelength range of 500 nm–1000 nm. The transmitted power was corrected by calculating the output power from the same structure but without gold NPs in order to eliminate the interference effect. The extinction is defined as $1 - T$, with T being the transmittance.

3. Results and discussion

3.1. Influences of NP height on the far-field and near-field optical responses of DNP array

Figure 2 shows the transmission spectra of DNP array with different values of NP height h but fixed parameters of $p = 470$ nm, $r = 60$ nm, and $g = 25$ nm. There is only one obvious transmission dip around the wavelength of 690 nm for each of the arrays with smaller height ($h < 110$ nm), whereas two transmission dips appear in the considered spectral range as the height is greater than 110 nm. The dip around 690 nm becomes more intense with the increase of NP height but its position is insensitive to the change of NP height, while that appearing at lower frequency shows red shift with the increase of h, suggesting a height-dependent optical response.

To understand the transmission characteristic caused by changing the NP height, we start with the investigation of resonance origin associated with these transmission dips. For a 2D nanostructure array, the lattice plasmon resonance arising from the coupling between the LSPR and the array diffraction order should be considered. For the first-order diffraction edge, its wavelength can be calculated by $\lambda_{\mathrm{glass}(1,0)} = d \times n_{\mathrm{glass}}$, where d is the grating constant and n_{glass} is the index of glass.[23] It occurs at 681 nm using $d = 470$ nm and $n_{\mathrm{glass}} = 1.45$, which is shown by the blue dashed line in Fig. 2. The transmission dip occurring on the long-wavelength side of the diffraction edge is a signature of coupling of light into an evanescent surface mode. Therefore, the spectral dip keeping fixed around 690 nm in the transmission spectra of DNP array with $p = 470$ nm (Fig. 2) corresponds to a lattice resonance caused by coupling of dimer's LSPR and array's first diffracted order. The LSPR is located around 560 nm for $h \geq 110$ nm and associated with the longitudinal coupling of the dipolar mode of two NPs.[6]

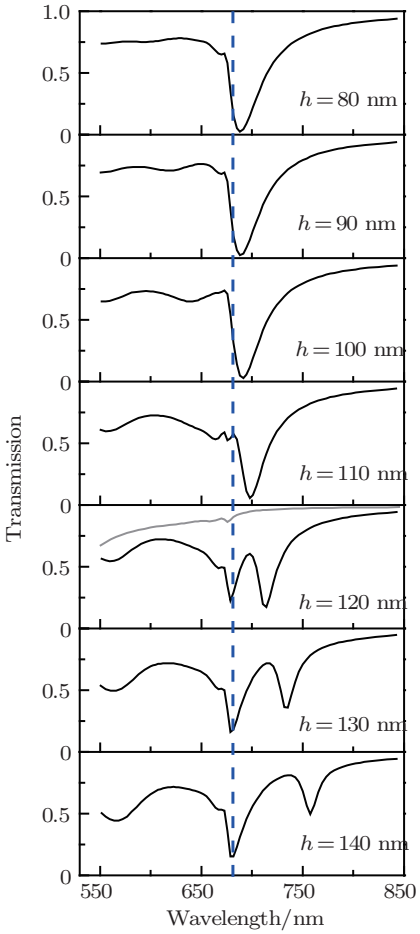


Fig. 2. (color online) Transmission spectra of a series of gold cylindrical DNP arrays with the NP height h varying from 80 nm (top line) to 140 nm (bottom line) in steps of 10 nm at normal-incidence with the polarization of E-field along the dimer axis. Other structural parameters are kept constant, i.e., $p = 470$ nm, $r = 60$ nm, and $g = 25$ nm. The vertical blue dashed line represents the wavelength position of the first-order diffraction edge. The dark black line in the column of $h = 120$ nm corresponds to the transmission spectra of the same array at normal-incidence with the polarization perpendicular to the dimer axis.

To give a direct insight into the transition of spectral profiles from one obvious resonance dip to two dips and understand the physics behind the height-dependent spectral features, we then investigate the near-field optical response of the DNPs arrays with different NP heights, which will demonstrate the involvement of out-of-plane magnetic resonance. Figure 3 shows the averaged enhancements of electric-field (blue line) and magnetic-field (black line) in the gap between two adjacent NPs, each as a function of the wavelength for the array with $h = 80$ nm, 100 nm, 120 nm and 140 nm, respectively. The averaged enhancement factor is defined as $\int_l |\boldsymbol{A}|\,\mathrm{d}l / \int_l |\boldsymbol{A}_0|\,\mathrm{d}l$, where A and A_0 represent the local electric field or magnetic field at a given position with and without the DNPs array, and l denotes the integration path indicated by the red dotted line in Fig. 1(b). In Fig. 3, we also present the corresponding extinction spectra (red dotted line) of the DNPs arrays for comparison of the simulated far-field and near-field optical responses.

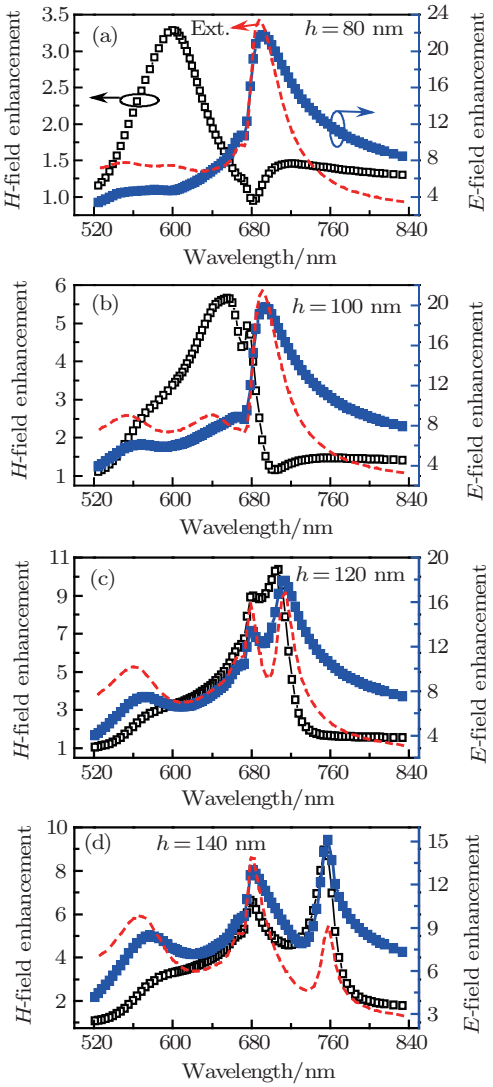


Fig. 3. (color online) Plots of averaged E-field (blue line with solid squares) and H-field (black line with open squares) enhancement ($\int_l |\boldsymbol{A}|\,\mathrm{d}l / \int_l |\boldsymbol{A}_0|\,\mathrm{d}l$) in the interparticle gaps versus wavelength for DNP arrays with different values of NP height ($h = 80$ nm, 100 nm, 120 nm, and 140 nm). Other structural parameters are kept constant, i.e., $p = 470$ nm, $r = 60$ nm, and $g = 25$ nm. The corresponding extinction spectra (red dotted line) of these DNP arrays are also provided here for comparisons.

Figure 3 indicates that the DNP array gives rise to both electric and magnetic field enhancements in the gap regions. There appears only one enhancement peak for each field occurring at different wavelengths with smaller NP height ($h =$ 80 nm). An obvious red shift of the magnetic field enhancement peak is observed as h increases from 80 nm to 100 nm. When the NP height further increases ($h > 110$ nm), both the electric and magnetic field enhancements split into two peaks and overlap. The electric or magnetic enhancement peak at 690 nm seems to be unchanged in position with the NP height while another exhibits remarkable red-shift with the further increase of h. The former is consistent with our above discussion about the lattice mode, and the latter displays the characteristics of LSPR due to the geometry-dependence. These indicate that both electric and magnetic resonances contribute to the

two transmission dips in Fig. 2. The sensitivity of the magnetic field enhancement peak (or the magnetic resonant frequency) to NP height can be understood based on the capacitive coupling of two adjacent NPs. By increasing the NP height and keeping other parameters constant, the capacitance between two adjacent NPs becomes larger, which will result in the decrease of magnetic resonant frequency ($f_{\rm m} \propto 1/\sqrt{LC}$).[32]

In terms of the spectral line shape exhibited in Fig. 3, the electric field enhancements present similar spectral features to the optical extinctions obtained in the far field, whereas the spectrum of H-field enhancement is inconsistent with that of extinctions for smaller NP height (Fig. 3(a) or Fig. 3(b)). This is because the magnetic resonance characterized by antiphase dipole oscillation in adjacent NPs has near-zero net dipole moment (also known as dark mode[33]), therefore presents an insignificant contribution to the far-field spectrum. Nevertheless, the averaged enhancement factor of magnetic field increases with NP height increasing and reaches the maximum of more than 10 till $h = 120$ nm and then declines as the height is further increased. Contrastively, the averaged electric field enhancement in the gap region decreases monotonically with h increasing from 80 nm to 160 nm.

Figures 4 illustrates the corresponding field distributions of E_z, $|E|$, and $|H|$ in the cut-plane through the dimer axis for DNP arrays with $h = 80$ nm and $h = 120$ nm at the peak wavelengths of averaged H-field or E-field enhancement. The field distributions of E_z are provided here due to the out-of-plane electric component responsible for the out-of-plane plasmon mode. For $h = 80$ nm, the out-of-plane anti-phase plasmon oscillation between two adjacent NPs is excited at $\lambda = 600$ nm (Fig. 4(a)), which corresponds to the antisymmetric magnetic mode and contributes to the H-field enhancement in gap region (Fig. 4(c) and Fig. 3(a)).[15,16] However, in-plane dipolar interaction between two particles dominates the optical response of DNP array at $\lambda = 690$ nm (the E_x distribution is not shown here), leading to the E-field enhancement in the gap (Fig. 4(e) and Fig. 3(a)). For DNP array with smaller NP height ($h = 80$ nm), the gaps between two adjacent NPs behave as hot spots of H-field or E-field at different excitation wavelengths (600 nm and 690 nm, respectively).

For the DNP array with $h = 120$ nm, the out-of-plane magnetic plasmon and the in-plane lattice resonance associated respectively with the H-field and the E-field enhancements can be excited simultaneously at both 679 nm and 711 nm (Fig. 3(c)). The two resonances carry fully the characteristics of both modes as shown in Figs. 4(h)–4(i) and Figs. 4(k)–4(l), suggesting the near-field interaction between them. Actually, the magnetic field of the lattice surface mode has the same direction as the induced magnetic moment of the magnetic resonance (along the y direction). Similar to two coupled dipoles giving rise to transverse coupling, the magnetic field of the lattice resonance can interact with that of the magnetic resonance in NP pairs, leading to two mixed modes, which can be explained based on the coupled oscillators model.[34] Simultaneous E-field and H-field enhancements can be achieved in the gaps at two resonance frequencies as the interaction between both modes occurs. In addition, quadrupole components are observed in the E-field distribution (Figs. 4(h) and 4(k)) due to the excitation of the multipole mode in a larger particle with higher NP.[35]

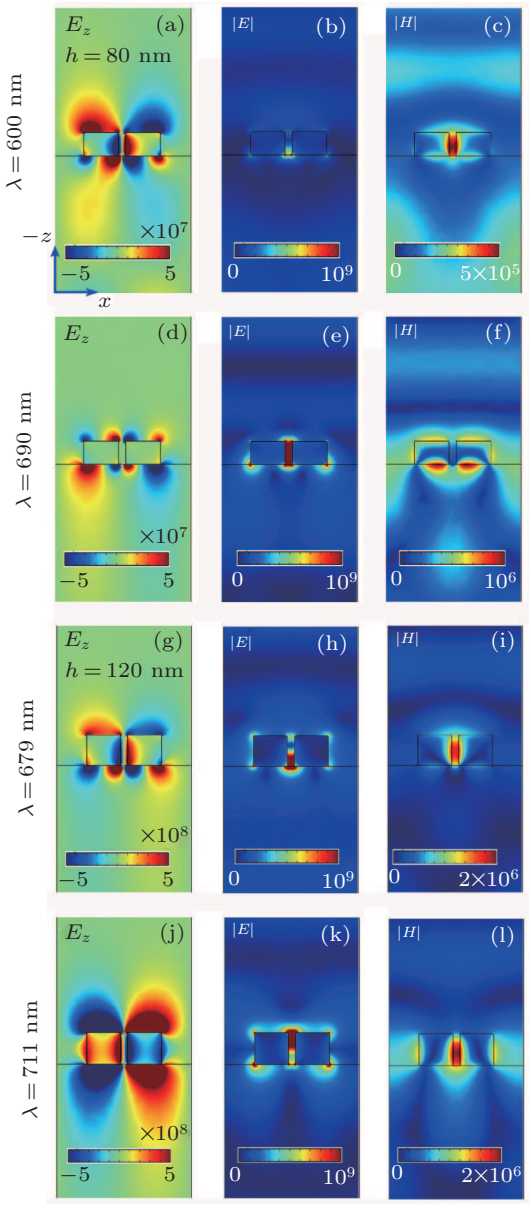


Fig. 4. (color online) Field distributions of $\boldsymbol{E}_z$, $|\boldsymbol{E}|$, and $|\boldsymbol{H}|$ in the x–z plane for the DNP array with different NP heights at the peak wavelengths of averaged H-field or E-field enhancement: (a)–(c), $h = 80$ nm and $\lambda = 600$ nm; (d)–(f), $h = 80$ nm and $\lambda = 690$ nm; (g)–(i), $h = 120$ nm and $\lambda = 679$ nm; (j)–(l), $h = 120$ nm and $\lambda = 711$ nm.

3.2. Tuning the optical response of DNP array through the periodicity

The interplay between out-of-plane magnetic plasmon and in-plane lattice resonance can be further explored by

investigating the influences of periodicity on far-field and near-field optical properties of DNP array with $h = 120$ nm. As illustrated in Fig. 5(a), there are two transmission dips for the array ($h = 120$ nm, $r = 60$ nm, and $g = 25$ nm) with a smaller period and only one for a larger period ($p \geq 500$ nm). The corresponding averaged H-field enhancement spectra indicates a noticeable weakening of the enhancement effect around the wavelength of 690 nm, accompanied by a negligibly small enhancement peak at the long wavelength as the array period exceeds 500 nm (Fig. 5(b)). The small H-enhancement peak is expected to be contributed by the induced H-field of the electric resonance. For the case of an averaged E-field enhancement, an obvious red-shift of one peak is observed as the periodicity increases (Fig. 5(c)). These phenomena can be understood very well by the fact that increasing the periodicity enables a linear red shift of the lattice resonance and consequently non-overlapping with the magnetic resonance, which can be confirmed by investigating the averaged near-field enhancement spectra of DNP array with $h = 80$ nm at different periodicities. As illustrated in Fig. 6(b), increasing the array period

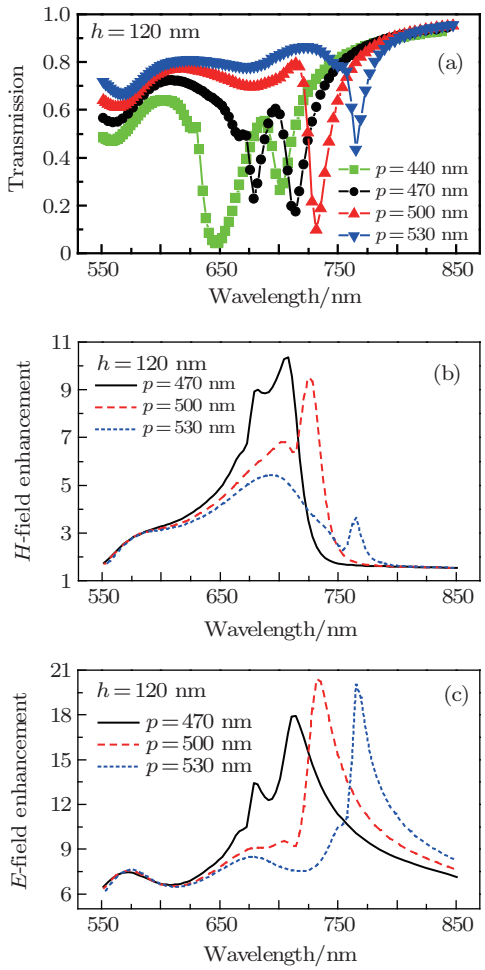


Fig. 5. (color online) Plots of transmission (a), averaged H-field (b), and E-field (c) enhancements versus wavelength for DNP array with different values of periodicity p and fixed structural parameters of $h = 120$ nm, $r = 60$ nm, and $g = 25$ nm.

leads to a linear red shift of E-field enhancement peak associated with the lattice resonance, but has negligible influence on the H-field enhancement peak caused by the out-of-plane magnetic plasmon. As a localized surface plasmon resonance (LSPR) mode, the out-of-plane magnetic resonance is strongly dependent on the geometrical structure of the DNP rather than the lattice period. The corresponding transmission spectra of DNP array with $h = 80$ nm but different periodicities are also provided in Fig. 6(a) for comparison. Therefore, the interplay between two plasmon modes due to their resonance overlapping can give rise to a remarkable spectral profile and optimum H-field enhancement effect in the gap region.

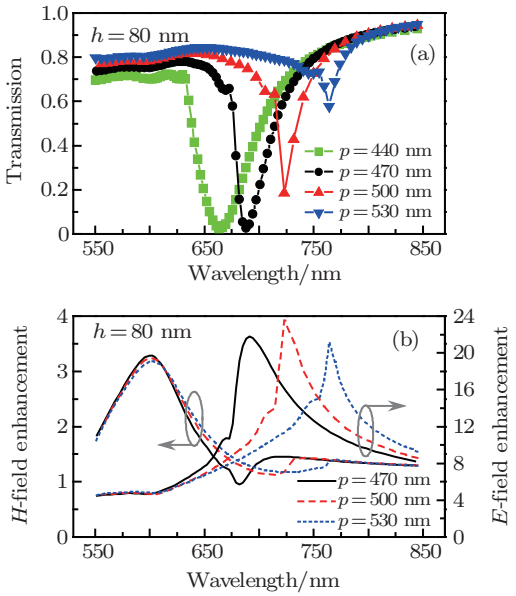


Fig. 6. (color online) Plots of transmission (a), averaged H-field and E-field (b) enhancements versus wavelength for DNP arrays with different values of periodicity p and fixed structural parameters of $h = 80$ nm, $r = 60$ nm, and $g = 25$ nm.

When the magnetic field of incident light is parallel to the dimer axis, no impressive spectral responses are observed because the out-of-plane magnetic resonance cannot be excited under this polarization configuration as shown by the dark black line in Fig. 2 for the array with $h = 120$ nm. In addition, we also demonstrate that a planar gold quadrumer array consisting of four identical nanocylinders arranged in a square configuration exhibits the similar optical responses as displayed in Figs. 2 and 3, independent of the incident polarization for symmetric configuration (not shown here). Moreover, the performances of H-field and E-field enhancements in the gap regions can be improved by further structural optimization, such as the interparticle distance, due to the magnetic and electric resonances of the nanoparticle pairs associated greatly with the coupling of two adjacent NPs.

4. Conclusion

In the present paper, we numerically demonstrate that the 2D DNP array supports the interplay between out-of-plane

magnetic plasmon and in-plane lattice resonance. The former can be tuned more easily over a larger wavelength range by controlling the NP height without changing the overall geometry of the nanostructure, whereas the latter depends greatly on array period. The interaction between the two plasmon modes can give rise to a remarkable change of the resonance lineshape and result in more than 10 times averaged H-field enhancement ($h = 120$ nm and $p = 470$ nm) in the gap region. Both the E-field and H-field hot spots appear simultaneously in the gap between neighboring particles at double resonance frequency as the interplay occurs, presenting potential applications in molecular detection and sensing. Our results not only offer an attractive way to tune the optical properties and achieve nano-localized electromagnetic field enhancements in plasmonic nanostructures, but also provide further insight into the plasmon interaction, especially for periodic nanostructures or metamaterials consisting of multiple large nanoparticles.

References

[1] Stewart M, Anderton C, Thompson L, Maria J, Gray S, Rogers J and Nuzzo R 2008 *Chem. Rev.* **108** 494
[2] Atwater H A and Polman A 2010 *Nat. Mater.* **9** 205
[3] Tong L M and Xu H X 2012 *Physics* **41** 582 (in Chinese)
[4] Cong C, Wu D J and Liu X J 2012 *Acta Phys. Sin.* **61** 047802 (in Chinese)
[5] Halas N J, Lal S, Chang W S, Link S and Nordlander P 2011 *Chem. Rev.* **111** 3913
[6] Rechberger W, Hohenau A, Leitner A, Krenn J, Lamprecht B and Aussenegg F 2003 *Opt. Commun.* **220** 137
[7] Pakizeh T, Dmitriev A, Abrishamian M S, Granpayeh N and Kall M 2008 *J. Opt. Soc. Am. B* **25** 659
[8] Grillet N, Manchon D, Bertorelle F, Bonnet C, Broyer M, Cottancin E, Lermé J, Hillenkamp M and Pellarin M 2011 *ACS Nano* **5** 9450
[9] Funston A M, Novo C, Davis T J and Mulvaney P 2009 *Nano Lett.* **9** 1651
[10] Oubre C and Nordlander P 2005 *J. Phys. Chem. B* **109** 10042
[11] Larsson E M, Hao F, Eurenius L, Olsson E, Nordlander P and Sutherland D S 2008 *Small* **4** 1630
[12] Hao E and Schatz G 2004 *J. Chem. Phys.* **120** 357
[13] Jain P K, Huang W Y and El-Sayed M A 2007 *Nano Lett.* **7** 2080
[14] Pelton M, Aizpurua J and Bryant G 2008 *Metal-nanoparticle Plasmonics Laser Photonics Rev.* **2** 136
[15] Pakizeh T, Abrishamian M, Granpayeh N, Dmitriev A and Käll M 2006 *Opt. Express* **14** 8240
[16] Grigorenko A N, Geim A K, Gleeson H F, Zhang Y, Firsov A A, Khrushchev I Y and Petrovic J 2005 *Nature* **438** 335
[17] Nordlander P 2013 *Nat. Nanotechnol.* 876-7
[18] Klein M W, Enkrich C, Wegener M and Linden S 2006 *Science* **313** 502
[19] Vourc'h E, Joubert P Y and Cima L 2009 *Prog. Electromagn. Res.* **99** 323
[20] Lamprecht B, Schider G, Lechner R, Ditlbacher H, Krenn J, Leitner A and Aussenegg F 2000 *Phys. Rev. Lett.* **84** 4721
[21] Singh R, Rockstuhl C and Weili Z 2010 *Appl. Phys. Lett.* **97** 241108
[22] Auguié B and Barnes W L 2008 *Phys. Rev. Lett.* **101** 143902
[23] Chu Y, Schonbrun E, Yang T and Crozier K B 2008 *Appl. Phys. Lett.* **93** 181108
[24] Giannini V, Vecchi G and Rivas J G 2010 *Phys. Rev. Lett.* **105** 266801
[25] Bitzer A, Wallauer J, Helm H, Merbold H, Feurer T and Walther M 2009 *Opt. Express* **17** 22108
[26] Kravets V, Schedin F and Grigorenko A 2008 *Phys. Rev. Lett.* **101** 87403
[27] Vecchi G, Giannini V and Gomez Rivas J 2009 *Phys. Rev. Lett.* **102** 146807
[28] Offermans P, Schaafsma M C, Rodriguez S R K, Zhang Y, Crego-Calama M, Brongersma S H and Gómez Rivas J 2011 *ACS Nano* **5** 5151
[29] Tang C, Zhan P, Cao Z, Pan J, Chen Z and Wang Z 2011 *Phys. Rev. B* **83** 041402
[30] Liu H, Sun X, Pei Y, Yao F and Jiang Y 2012 *Opt. Lett.* **36** 2414
[31] Johnson P and Christy R 1972 *Phys. Rev. B* **6** 4370
[32] Ding P, Liang E J, Hu W Q, Zhou Q, Zhang L, Yuan Y X and Xue Q Z 2009 *Opt. Express* **17** 2198
[33] Maier S A 2011 *Laser Focus World* **47** 63
[34] Ding P, Fan C Z, Cheng Y G, Liang E J and Xue Q Z 2012 *Appl. Opt.* **51** 1879
[35] Henson J, DiMaria J and Paiella R 2009 *J. Appl. Phys.* **106** 093111